Chaos

A combined method to estimate parameters of the thalamocortical model from a heavily noise-corrupted time series of action potential

Cite as: Chaos **24**, 013128 (2014); https://doi.org/10.1063/1.4867658
Submitted: 17 April 2013 . Accepted: 22 February 2014 . Published Online: 05 March 2014

Ruofan Wang, Jiang Wang, Bin Deng, Chen Liu, Xile Wei, K. M. Tsang, and W. L. Chan

CHAOS **24**, 013128 (2014)

A combined method to estimate parameters of the thalamocortical model from a heavily noise-corrupted time series of action potential

Ruofan Wang,[1] Jiang Wang,[1] Bin Deng,[1,a)] Chen Liu,[1] Xile Wei,[1] K. M. Tsang,[2] and W. L. Chan[2]
[1]*Department of Electrical and Automation Engineering, Tianjin University, Tianjin, China*
[2]*Department of Electrical Engineering, The Hong Kong Polytechnic University, Kowloon, Hong Kong*

(Received 17 April 2013; accepted 22 February 2014; published online 5 March 2014)

A combined method composing of the unscented Kalman filter (UKF) and the synchronization-based method is proposed for estimating electrophysiological variables and parameters of a thalamocortical (TC) neuron model, which is commonly used for studying Parkinson's disease for its relay role of connecting the basal ganglia and the cortex. In this work, we take into account the condition when only the time series of action potential with heavy noise are available. Numerical results demonstrate that not only this method can estimate model parameters from the extracted time series of action potential successfully but also the effect of its estimation is much better than the only use of the UKF or synchronization-based method, with a higher accuracy and a better robustness against noise, especially under the severe noise conditions. Considering the rather important role of TC neuron in the normal and pathological brain functions, the exploration of the method to estimate the critical parameters could have important implications for the study of its nonlinear dynamics and further treatment of Parkinson's disease.
[http://dx.doi.org/10.1063/1.4867658]

To explore the time-varying dynamic properties of a thalamocortical (TC) neuron model that could characterize the Parkinsonian state, it is necessary to adapt some undetermined coefficients of this nonlinear model to observed data. Like other neural models, since some of variables and parameters of TC model cannot be measured directly, the reliable reconstruction of variables and parameters using only a small portion of noise-corrupted observed data, such as the time series of action potentials, is one of the most meaningful research topics in neurological disease treatment. Currently, several algorithms based on synchronization have been successfully applied to determine the unfixed parameters. However, these algorithms can only be used in models with weak nonlinearities or small amounts of noise. The unscented Kalman filter (UKF) technique enables simultaneous state and parameter estimation from data with relatively large amounts of observation noise. However, it should be noted that UKF considers unknown parameters as virtual states of a joint system, so the accuracy of parameter estimation will not be very high. Thus, this paper combines the UKF and the synchronization-based estimation approach to estimate the unknown parameters of the nonlinear TC model from heavily noise-corrupted time series of action potentials. It can be verified that such combined estimation approach has beneficial effects in reconstructing the entire set of TC parameters accurately, rapidly and it is robust to strong observation noise. The success must be related to the intrinsic independence of ionic currents and time constants presented in these equations, and in the real thalamocortical neuron upon which they are based.

I. INTRODUCTION

Parkinson's disease (PD)[1,2] is a degenerative neurological condition, which is caused by dopamine depletion in the basal ganglia (BG)[3–7] and characterized by a host of motor and cognitive dysfunctions. In the Parkinsonian state, the dynamics of thalamocortical neuron, a relay station whose physiological role is to respond faithfully to incoming sensorimotor signals, is blocked. It has been demonstrated that the deep brain stimulation (DBS)[8–13] at high frequencies between 130 Hz and 180 Hz is clinically effective in the treatment of PD, by functionally restoring TC relay activity.[14–16] It is thus suggested that TC neurons is important for investigating the underlying mechanism of normal and PD behaviors in the brain.

By now, many computational models have been proposed to investigate both the physiological role and pathological behavior of TC neurons. Recently, Rubin and Terman have developed a TC model consisted of several synaptic connections and ionic channels.[17] Based on this model, Feng *et al*. have proposed a novel closed-loop global optimization algorithm which is more effective than the prior high-frequency open-loop DBS counterparts.[13] Moreover, Liu *et al*. have investigated a BG network composed of Hodgkin–Huxley (HH) spiking neurons and found that the rhythmic/oscillatory patterns that characterize a dopamine-depleted condition can be suppressed by a direct control of BG neurons in the network.[3] However, in all these studies, the values of model parameters are set empirically, which is

[a)]Author to whom correspondence should be addressed. Electronic mail: dengbin@tju.edu.cn. Fax/Tel.: 86-22-27402293

unrealistic. In fact, only the membrane potential of TC neuron can be observed in physiological experiments, and noise is inevitable and usually strong. In neural systems, the source of noise is various, such as random opening and closing of ionic channels, the synaptic connections to the neuron and observation noise in the voltage-clamp experiment, and so on. All these noise may lead to a dramatic effect on neuronal behavior, inducing limit cycles on otherwise stable dynamics. In order to further explore precise dynamics of the TC neuron and achieve a DBS closed-loop control strategy, it is a significant challenge to estimate the unknown parameter in a nonlinear dynamical neural model with the strong observed data.[18–22]

In previous works, we have investigated the parameter estimation based on the synchronization and adaptive control.[23–31] The proposed method can rapidly and accurately respond to the changes of undetermined parameters via the synchronization of the experiment and auxiliary systems. However, it can only robust against weak noise and may lose control when the noise is strong enough for itself nonlinear dynamics. The UKF[32–38] method can exactly solve this kind of noise problem by filtering the noises out. In addition, UKF removes the requirement to explicitly calculate Jacobians, which may be a difficult task for complex functions. Thus, UKF can complete the recursion and update of the state and the errors by the covariance with less computational complexity through a nonlinear transformation. In this work, we proposed a combined method composing of the UKF technique and the synchronization-based method to estimate the unknown parameters of the TC neuron model.[23] The advantage of this control algorithm is guaranteeing a high accuracy of parameter estimation even when the observations are noise-corrupted.

Accordingly, the subsequent parts of this paper are organized as follows: in Sec. II, we give a brief description of the TC model; in Sec. III, we formulate the synchronization-based and the combined estimation method in detail; numerical results of the TC model obtained by the combined method from heavily noise-corrupted time series of action potential are presented in Sec. IV, which is followed by conclusions in Sec. V.

II. THE THALAMOCORTICAL MODEL

TC model can illustrate ionic channel properties and synaptic connections, which is more to understand the physiological mechanisms of PD characterized by loss of TC relay neuron's reliability. As shown in Fig. 1, the single TC neuron receives inhibitory inputs from the basal ganglia as well as periodic excitatory inputs from the cortex. The "+" and "−" in Fig. 1 indicate excitatory and inhibitory synaptic connections, respectively.

As shown in Fig. 2, the responses of the TC neuron to the external afferent signals are different under the normal state and Parkinsonian state. Under the normal state, the TC relay neuron can respond to the excitatory periodic sensorimotor input from the cortex faithfully, namely, a current pulse can induce only a spike of TC neuron within a small time window with a certain degree of confidence (Fig. 2(a)).

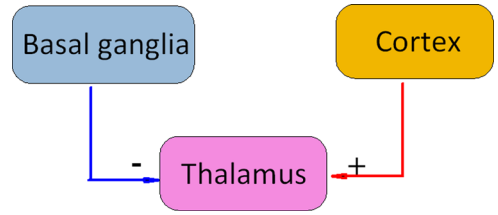

FIG. 1. The functional links of the thalamus, the basal ganglia, and the cortex.

While under the Parkinsonian state, the fidelity of the TC relay neuron is compromised by the enhanced inhibitory synaptic connection from the basal ganglia. The TC neuron is too over-inhibited to respond to the cortex input faithfully anymore, sometimes along with spike failure and rebound bursting (Fig. 2(b)). Thus, the TC neuron is not only a simple relay center for signals anymore but also can be served as an indicator to identify whether in Parkinsonian state or not.

The voltage of TC relay neuron is modeled via

$$C_m \frac{dv_{Th}}{dt} = -I_L - I_{Na} - I_K - I_T - I_{Gi\to Th} + I_{SM}, \qquad (1)$$

where v_{Th} represents the membrane potential. We assume that the membrane capacitance C_m is unity. I_L, I_{Na}, I_K, and I_T represent the passive leak, sodium, potassium, and low-threshold T-type Ca^{2+} current, respectively. $I_{Gi\to Th}$ is the synaptic current from BG to TC neuron, and I_{SM} is the periodic excitatory input from the sensorimotor cortex. To reflect more closely the actual signals from the cortex, we substitute a periodic square wave with stochastic noise for the periodic sensorimotor input employed in the TC neuron model in the previous literature[1,6,11,16]

$$I_{SM} = A_{SM} H\left(\sin\left(\frac{2\pi t}{\rho_{SM}}\right)\right)\left(1 - H\left(\sin\left(\frac{2\pi t + D_{SM}}{\rho_{SM}}\right)\right)\right) + noise, \qquad (2)$$

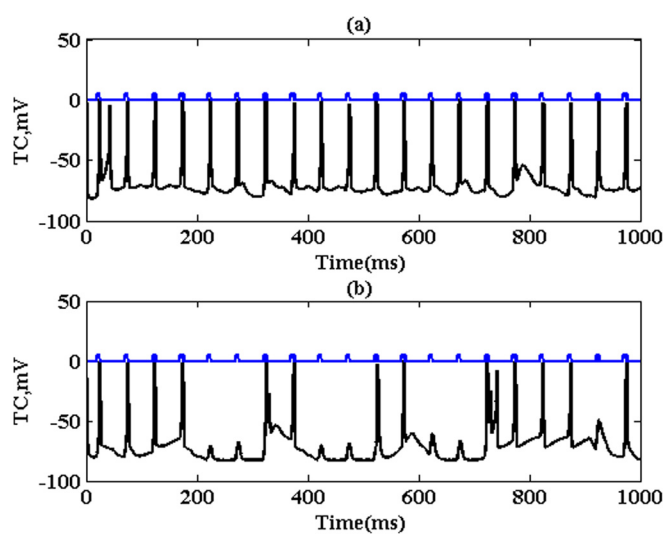

FIG. 2. Discharge properties of TC neuron in the input of the periodic sensorimotor current. (a) Discharge properties of the normal TC neuron. (b) Discharge properties of TC neuron under Parkinsonian state.

where ρ_{SM}, D_{SM}, and A_{SM} are the period, duration, and amplitude of I_{SM}, respectively. H is the Heaviside step function, such that, $H(x) = 0$ if $x < 0$ and $H(x) = 1$ if $x > 0$.

The ionic currents are given by

$$\begin{aligned} I_L &= g_L(v_{Th} - E_L), \\ I_{Na} &= g_{Na} m_\infty^3(v_{Th}) h_{Th}(v_{Th} - E_{Na}), \\ I_K &= g_K[0.75(1 - h_{Th})]^4(v_{Th} - E_K), \\ I_T &= g_T p_\infty^2(v_{Th}) \omega_{Th}(v_{Th} - E_T), \end{aligned} \tag{3}$$

where g_i and E_i term with $i \in \{K, Na, L, T\}$ are the maximum channel conductance expressed in $\mathrm{mS/cm^2}$ and reversal potentials expressed in mV for the ion i, respectively. $p_\infty(v_{Th})$ and ω_{Th} are the T-current gating variable and inactivation variable, respectively. The underlying ionic mechanism beyond the rebound behavior of the TC neuron in the Parkinsonian state is relevant to the slow, low-threshold T-type Ca^{2+} current in Eq. (3). $X_\infty \in \{m_\infty, h_\infty, p_\infty, \omega_\infty\}$ represents the voltage-sensitive steady-state function and $\tau_x \in \{\tau_h, \tau_\omega\}$ represents the time constant of channel, which are expressed as follows:

$$\begin{aligned} m_\infty(v_{Th}) &= \frac{1}{1 + \exp\left(-\dfrac{v_{Th} + 37}{7}\right)}, \\ h_\infty(v_{Th}) &= \frac{1}{1 + \exp\left(\dfrac{v_{Th} + 41}{4}\right)}, \\ p_\infty(v_{Th}) &= \frac{1}{1 + \exp\left(-\dfrac{v_{Th} + 60}{6.2}\right)}, \\ \omega_\infty(v_{Th}) &= \frac{1}{1 + \exp\left(\dfrac{v_{Th} + 84}{4}\right)}, \\ \tau_h(v_{Th}) &= \frac{1}{a_h(v_{Th}) + b_h(v_{Th})}, \end{aligned} \tag{4}$$

where $a_h(v_{Th}) = 0.128 \cdot \exp\left(-\frac{v_{Th}+46}{18}\right), b_h(v_{Th}) = \frac{4}{1+\exp\left(-\frac{v_{Th}+23}{5}\right)}$.

Thus, the inactivation variables follow the Hodgkin-Huxley formalism with first-order dynamics

$$\begin{aligned} \frac{dh_{Th}}{dt} &= \frac{h_\infty(v_{Th}) - h_{Th}}{\tau_h(v_{Th})}, \\ \frac{d\omega_{Th}}{dt} &= \frac{\omega_\infty(v_{Th}) - \omega_{Th}}{\tau_\omega(v_{Th})}. \end{aligned} \tag{5}$$

In this nominal TC model, the parameters E_i and g_i, $i \in \{K, Na, L, T\}$ are set as $E_K = -90$, $g_K = 5$, $E_{Na} = 50$, $g_{Na} = 3$, $E_L = -70$, $g_L = 0.05$, $E_T = 120$, $g_T = 5$ similar to the values proposed by Rubin and Terman.[17] However, in the individual TC neuron, some parameters are actually undetermined. To simplify the problem, without loss of generality, we just assume parameter λ as an unknown constant, with the other parameters known. Similarly, the other unknown parameters can be estimated with the same method. In this research, we estimate parameters of the low-threshold T-type Ca^{2+} channel in Eq. (3) using the combined method proposed in Sec. III.

III. THE COMBINED METHOD FOR PARAMETER ESTIMATION

A. The estimation method based on synchronization

Assuming that the number of independent variables and the structure of underlying dynamical equations for a chaotic system are known, it is proved rigorously that all unknown parameters can be estimated dynamically from time series of the experimental system by adopting the invariance principle of differential equations.

First, we consider the noise-free experimental system as

$$\dot{x} = F(x, \lambda, t), \tag{6}$$

where $x = (x_1, x_2, ..., x_n) \in R^n$ is the state vector without noise, $F(x, \lambda, t) = (F_1(x, \lambda, t), F_2(x, \lambda, t), ..., F_n(x, \lambda, t),)$ is a nonlinear vector function with $F_i(x, \lambda, t) = g_i(x, t) + \sum_{j=1}^m \lambda_{ij} f_{ij}(x, t), i = 1, 2, ...n$. Here, $g_i(x, t)$ and $f_{ij}(x, t)$ are nonlinear functions, and $\lambda = \lambda_{ij} \in U \subset R^{nm}$ are unknown parameters to be estimated. U is a bounded set.

Furthermore, the form of this model satisfies two premises assumptions which are necessary for the following estimation.

- Assumption 1: All parameters satisfy the requirement of parameter linearization, which means for each parameter the model can be described as $\dot{x} = g(x) + \lambda \cdot f(x)$.
- Assumption 2: $g(x)$ and $f(x)$ in functions $\dot{x} = g(x) + \lambda \cdot f(x)$ are Lipschitzian, which means there exists $L_1, L_2 \in R^+$, so that

$$\begin{cases} \|f(x_1) - f(x_2)\| \le L_1 \|x_1 - x_2\| \\ \|g(x_1) - g(x_2)\| \le L_2 \|x_1 - x_2\|, \end{cases} \tag{7}$$

  where $L_1, L_2 \in R^+$ refers to the uniform Lipschitz constant.

It is assumed that time series for all variables of Eq. (6) are available. To estimate all unknown parameters λ from these time series, we introduce an auxiliary system of variables $y = (y_1, y_2, ..., y_n)$, whose evolution equations have the identical form to that of x. But the corresponding parameters are not the same, which will be set to arbitrary initial values, that is, $q = q_{ij}, i = 1, 2, ..., n,\ j = 1, 2, ..., m$. In contrast to the experimental system (6), the auxiliary system can be controlled by adding a simple linear feedback control input. The auxiliary system is given by the following equation:

$$\dot{y} = F(x, q, t) + u, \tag{8}$$

where u is the external stimulus, which can be described by the following equation:

$$u_i = \varepsilon_i \cdot e_i, \tag{9}$$

where $e_i = y_i - x_i$ is the synchronization error of systems (6) and (8). The feedback strength $\varepsilon = (\varepsilon_1, \varepsilon_2, ..., \varepsilon_n)$ will be adaptively varied according to the following update law:

$$\dot{\varepsilon}_i = -\alpha_i \cdot e_i^2, \quad i = 1, 2, ..., n, \tag{10}$$

where $\alpha_i > 0, i = 1, 2, ..., n$ are arbitrary constants.

The equations governing the evolution of the parameters q are chosen similar to the adaptive controller and have the form

$$\dot{q}_{ij} = -\beta_{ij} \cdot e_i \cdot f_{ij}(y,t), \quad i = 1,2,...,n, \quad j = 1,2,...,m, \quad (11)$$

where $\beta_{ij} > 0, i = 1,2,...n, j = 1,2,...,m$ are arbitrary constants. Because the unknown parameter λ_i to be estimated is a constant, under the more rigorous condition, the system (7) can be rewritten as

$$\dot{x} = F(x,\lambda,t), \quad \dot{\lambda} = 0. \quad (12)$$

One of the central questions concerned with chaos synchronization of the two systems is the strict stability of the identical behavior. In summary, in the restrictions of Eqs. (8), (9), (11), and (12), we introduce the non-negative Lyapunov function

$$V = \frac{1}{2}\left[\sum_{i=1}^{n} e_i^2 + \sum_{i=1}^{n}\sum_{j=1}^{m}\frac{1}{\beta_{ij}}(q_{ij}-\lambda_{ij})^2 + \sum_{i=1}^{n}\frac{1}{\alpha_i}(\varepsilon_i + L)^2\right], \quad (13)$$

where $L > nl$. By differentiating the Lyapunov function V of the system, we can obtain

$$\begin{aligned}
\dot{V} &= \sum_{i=1}^{n} e_i \cdot (\dot{y}_i - \dot{x}_i) + \sum_{i=1}^{n}\sum_{j=1}^{m}\frac{1}{\beta_{ij}}(q_{ij}-\lambda_{ij}) \cdot \dot{q}_{ij} + \sum_{i=1}^{n}\frac{1}{\alpha_i}(\varepsilon_i + L) \cdot \dot{\varepsilon}_i \\
&= \sum_{i=1}^{n} e_i \cdot \left[F_i(y,q,t) - F_i(x,\lambda,t) + \varepsilon_i \cdot e_i\right] - \sum_{i=1}^{n}\sum_{j=1}^{m}(q_{ij}-\lambda_{ij}) \cdot e_i \cdot f_{ij}(y) - \sum_{i=1}^{n}(e_i + L)e_i^2 \\
&= \sum_{i=1}^{n} e_i \cdot \left[F_i(y,q,t) - F_i(x,\lambda,t)\right] - \sum_{i=1}^{n} e_i \cdot \left[F_i(y,q,t) - F_i(y,\lambda,t)\right] - L\sum_{i=1}^{n} e_i^2 \\
&= \sum_{i=1}^{n} e_i \cdot \left[F_i(y,q,t) - F_i(x,\lambda,t)\right] - L\sum_{i=1}^{n} e_i^2 \\
&\le \sum_{i=1}^{n} e_i \cdot l \cdot \max_{1\le j\le m}|e_j| - L\sum_{i=1}^{n} e_i^2 \le (nl - L)\sum_{i=1}^{n} e_i^2 \\
&\le 0.
\end{aligned}$$

It is obvious that $\dot{V} = 0$ if and only if $e_i = 0$, $i = 1,2,...,n$. Therefore, the set $E = \{e = 0, \lambda - q = 0, \varepsilon = \varepsilon_0 \in R^n\}$ is the largest invariant set contained in $\dot{V} = 0$ for the system. In brief, the synchronization parameter estimation method can be expressed as: starting with arbitrary initial values, the undetermined parameters λ of the experimental system can be asymptotically approximated to the fixed value q of the auxiliary system as soon as the two systems achieve synchronization, when applying an external stimulus input to the auxiliary system.

This method which is able to estimate more than one parameter simultaneously can stay stable even when all parameters are undetermined. Besides, such estimation is quite robust against the weak noise and able to respond rapidly to changes in operating parameters of the experimental system.

However, the synchronization-based method is only robust against weak observation noise which can be seen as an external disturbance. When the observation noise intensity increases, it may lose efficacy in particular for the nonlinear dynamics. Thus, in the heavily noise-corrupted TC system, it is unsuitable to adopt the above method to estimate the unknown parameters directly.

B. The combined method

Considering the strong noise of the TC neural system, the combined parameter estimation method, which summarizes the advantages of both the synchronization-based method and UKF, is adopted to estimate unfixed parameters. The proposed method can be depicted as follows: first, UKF is employed to estimate all the state variables of the experimental system from the noise-corrupted data observed. Second, the estimated state variables $\hat{x}_i(t|t)$ obtained through the UKF method are used as the driven signals to drive the auxiliary systems (8)–(11) to synchronize to experimental system (6). Finally, the unknown parameters λ may be dynamically estimated from q in the auxiliary system precisely and rapidly. Thus, the linear feedback control input u in Eq. (9) can be transformed into the following form which is the key core of the combined method for the parameter estimation:

$$u = \varepsilon_i \cdot (y_i - \hat{x}_i(t|t)), \quad (14)$$

where $\hat{x}_i(t|t)$ is the estimation value of the membrane potential at time t, which is obtained from the membrane potential at time $t - \Delta t$ by the UKF updating formula.

In general, UKF works as follows. For a n-dimensional estimated state $\hat{x}$, the UKF generates $2n$ sigma points $\{\chi_i\}_0^{2n}$ whose elements are $\chi_i = \hat{x} \pm \sqrt{nP}$, where P is the estimated covariance matrix of estimation errors of the state $\hat{x}$. Sigma points can be regarded as sample points at the boundaries of a covariance ellipsoid. The core computing of the UKF algorithm can be described as follows:

$$\begin{aligned}\chi_i\big(t|(t-\Delta t)\big) &= f\big(\chi_i\big((t-\Delta t)|(t-\Delta t)\big),\lambda,u\big),\\ \gamma_i\big(t|(t-\Delta t)\big) &= h\big(\chi_i\big(t|(t-\Delta t)\big)\big),\end{aligned} \tag{15}$$

where f is the nonlinear function of the state, which can make the sigma points $\{\chi_i\}_0^{2n}$ estimated at $t-\Delta t$ iterate forward to the values estimated at t. Then the sigma points are further transformed by the observation function h to generate the estimation of the next measurement. Moreover, the notation $X\big(k|(k-1)\big)$ indicates the value of the quantity X at time k using information taken up to time $k-1$. Likewise, $X(k|k)$ indicates the value of X computed at time k using the information available up to and including time k.

The estimation of the system state $\hat{x}\big(t|(t-\Delta t)\big)$ and the system $\hat{y}\big(t|(t-\Delta t)\big)$ can be obtained by weighing the resulting sample sets $\big\{\chi_i\big(t|(t-\Delta t)\big)\big\}_0^{2n}$ and $\big\{\gamma_i\big(t|(t-\Delta t)\big)\big\}_0^{2n}$, depicted as the following equation:

$$\begin{aligned}\hat{\mathbf{x}}\big(t|(t-\Delta t)\big) &= \sum_{i=0}^{2n} W_i\cdot\chi_i\big(t|(t-\Delta t)\big),\\ \hat{\mathbf{y}}\big(t|(t-\Delta t)\big) &= \sum_{i=0}^{2n} W_i\cdot\gamma_i\big(t|(t-\Delta t)\big),\end{aligned} \tag{16}$$

where $W_i=\frac{1}{2(n+\kappa)}, i=1,2,...,2n$ is the weight.

Then we define the prior covariance matrix of the ensemble members $P_{xx}(t|(t-\Delta t))$, $P_{yy}(t|(t-\Delta t))$, $P_{xy}(t|(t-\Delta t))$ as follows:

$$\begin{aligned}P_{xx}\big(t|(t-\Delta t)\big) &= \sum_{i=0}^{2n} W_i\big[\chi_i\big(t|(t-\Delta t)\big)-\hat{x}_i\big(t|(t-\Delta t)\big)\big]\\ &\quad\times\big[\chi_i\big(t|(t-\Delta t)\big)-\hat{x}_i\big(t|(t-\Delta t)\big)\big]^T,\\ P_{yy}\big(t|(t-\Delta t)\big) &= \sum_{i=0}^{2n} W_i\big[\gamma_i\big(t|(t-\Delta t)\big)-\hat{y}_i\big(t|(t-\Delta t)\big)\big]\\ &\quad\times\big[\gamma_i\big(t|(t-\Delta t)\big)-\hat{y}_i\big(t|(t-\Delta t)\big)\big]^T,\\ P_{xy}\big(t|(t-\Delta t)\big) &= \sum_{i=0}^{2n} W_i\big[\chi_i\big(t|(t-\Delta t)\big)-\hat{x}_i\big(t|(t-\Delta t)\big)\big]\\ &\quad\times\big[\gamma_i\big(t|(t-\Delta t)\big)-\hat{y}_i\big(t|(t-\Delta t)\big)\big]^T.\end{aligned} \tag{17}$$

In Eq. (17), the covariance matrix P depicts the estimation errors of the state $\hat{x}$. Taking P_{xx}, for example, minimizing the trace of the matrix P_{xx} minimizes the sum variances of the individual components of the state x, and this will generate the best Kalman gain matrix K.

So the clean state $\hat{x}_i(t|t)$ can be obtained from the noise-corrupted state $\hat{x}_i\big(t|(t-\Delta t)\big)$ by using the UKF updating formula

$$\begin{aligned}K(t) &= P_{xy}\big(t|(t-\Delta t)\big)\cdot P_{yy}^{-1}\big(t|(t-\Delta t)\big),\\ \hat{x}(t|t) &= \hat{x}\big(t|(t-\Delta t)\big)+K(t)\cdot\big[y(t)-h\big(\hat{x}\big(t|(t-\Delta t)\big)\big)\big],\\ P(t|t) &= P\big(t|(t-\Delta t)\big)-K(t)\cdot P_{yy}\big(t|(t-\Delta t)\big)\cdot K^T(t),\end{aligned} \tag{18}$$

where K is the Kalman gain matrix. However, the unknown parameters are considered as extra state variables which may decrease the accuracy in the UKF.

Obviously, the combined estimation approach is quite robust against the observation noises. In comparison to other parameter estimation methods, the distinguishing characters of this method are as follows: (i) it can be applied to the nonlinear TC neuron which is heavily corrupted with noise; (ii) it is analytical and rigorous because it does not require one to numerically determine any additive parameters; (iii) it is systematic because the control technique in the form of Eqs. (8)–(10) and (16) can be applied to all chaotic systems satisfying the uniform Lipschitz condition.

IV. RESULTS

Assuming we have known the nominal functional form of the TC model, we can consider the unknown parameters as virtual states in need of estimation. The joint system can be written in the following forms:

$$\begin{aligned}x(t) &= f\big(x(t-\Delta t),\lambda(t-\Delta t)\big)(\Delta t>0),\\ \lambda(t) &= \lambda(t-\Delta t),\\ y(t) &= h(x(t))+r(t),\end{aligned} \tag{19}$$

where $x(t)=(x_1,x_2,x_3)$, $\lambda(t)=(\lambda_1,\lambda_2,\lambda_3)$, $\Delta t=0.01$, $r(t)$ is the observation noise injected in the voltage which can improve the computational efficiency. f denotes the TC model equation which is solved by the four-order Runge-Kutta method. Because only the membrane potential can be measured, h is set as $h=\begin{pmatrix}1 & 0 & 0\end{pmatrix}$. The observations are generated by adding white Gaussian noise whose intensity is $D=0.1$ to the membrane potential

Under the assumption that TC model functional form and observation noise are known, we first adopt the UKF method to estimate the state of the joint system by filtering the noise out. The initial state is set to be $\hat{x}=\begin{pmatrix}-65 & 0.1 & 0.1\end{pmatrix}$, and the initial guess for parameter values is chosen as $\lambda_i=\begin{pmatrix}-150 & 0 & 30 & 0 & -100 & 0 & 100 & 0\end{pmatrix}$ with $i\in\{E_K\ g_K\ E_{Na}\ g_{Na}\ E_L\ g_L\ E_T\ g_T\}$. The membrane potential corrupted with noise and the noise-free state are drawn in Fig. 3(b) by blue and red lines, respectively. It is assumed that the noise-free state can be obtained under the ideal observation condition as a reference value. Compared to the differences between noise-free data and noisy data with the maximum amplitude about 2mV in Fig. 3(b), the differences between the estimated and the noise-free states as shown by blue and red traces in Fig. 3(d) are nearly one tenth, which proved the validity of the UKF estimation algorithm. Shown in Fig. 3(a), the trajectory of the noise-free attractor in the phase-space indicates the dynamic characteristics of the fast and slow variables, which corresponds to the noise-free time series of the action potential in Fig. 3(b), while Fig. 3(c) is the trajectory of the estimated attractor in the phase-space, corresponding to the periodic discharge of the estimated time series in Fig. 3(d).

Then, the time series estimated by the UKF above are brought into the synchronization-based estimation system in order to estimate the unknown parameters of the TC model. The various parameters of all ion channels in Eq. (3) have been estimated. We just take the reversal potentials and the maximum channel conductance of the low-threshold T-type

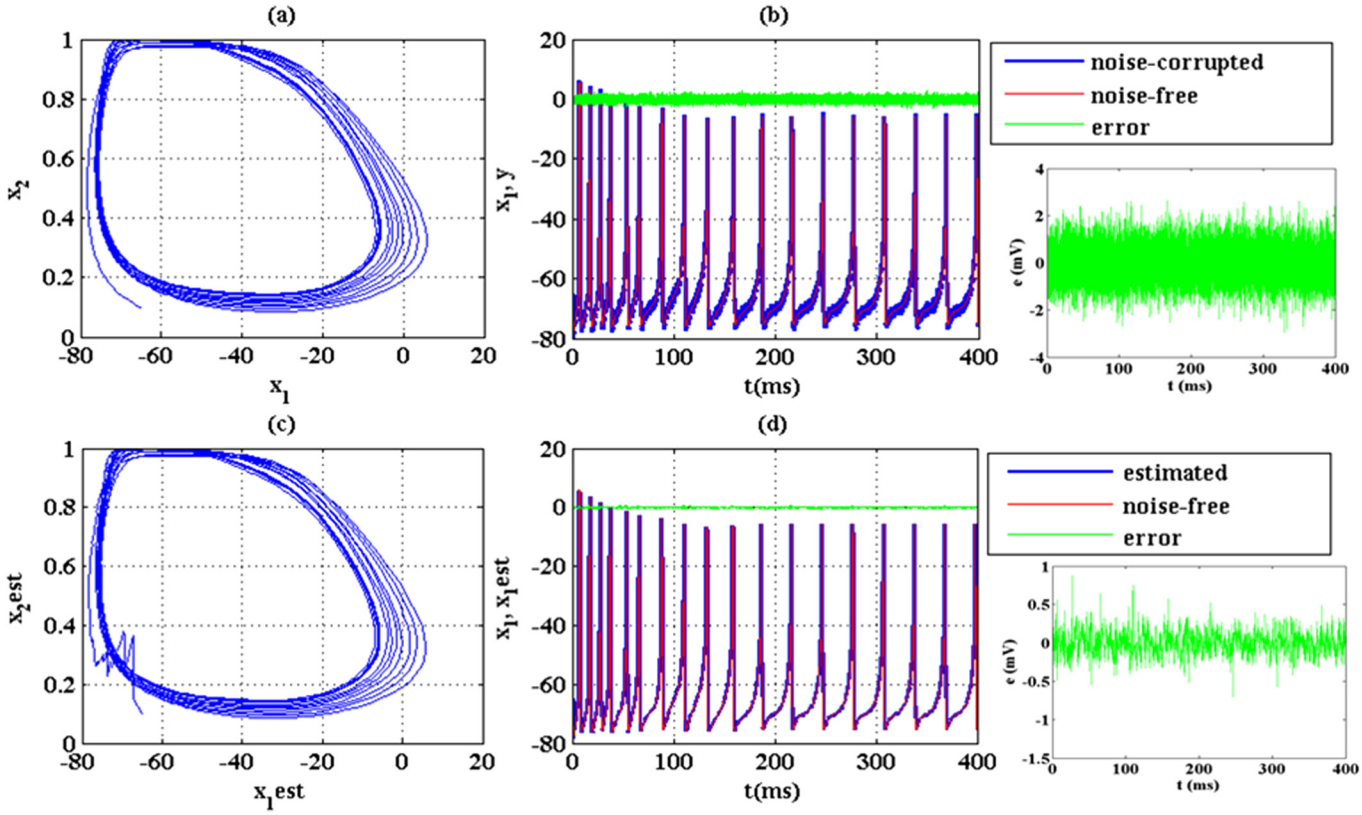

FIG. 3. (a) Clean attractor for TC model. (b) Noisy-free (red) and noisy observation (blue) for this limit cycle. (c) Estimated attractor for TC model. (d) Noisy-free (red) and estimated observation (blue) for this limit cycle.

Ca^{2+} channel as examples. The low-threshold T-type Ca^{2+} reversal potentials are shown in Fig. 4, where the blue, red, and black lines indicate the combined method, the UKF, and the synchronization-based method, respectively.

Fig. 4(a) describes the estimation dynamic results when the noise intensity $D = 0.1$. It should be noticed that although in the combined method, the response speed may be slightly slower than the synchronization-based method owing to the iteration process of the UKF algorithm, the parameters estimated can converge to the true values more smoothly and precisely than that in the other two estimation methods. While only using the UKF method will result in fluctuations in the convergence process, which means the accuracy is low, and in the convergence progress, the synchronization method shows a noticeable decreasing trend. The detailed dynamic description after convergence in the last 50 ms of the simulation can be clearly observed in the inset chart.

In order to further quantitatively compare the dynamic convergence process of these three methods, we calculate the average value and variance after converged, represented as the histograms and the error bars in Fig. 4(b). It is noted that the average value estimated by the combined method is the closest to the true value 120, and the error bar is the shortest corresponding to the minimum fluctuation. The difference between the estimated value and the expected value in the synchronization-based method is the maximum, and the fluctuation is dramatic. The results of UKF are intermediate.

For the purpose of studying the influence of the observation noise intensity D on the accuracy of the parameter estimation, we introduce the normalized absolute error of λ as $A_i = |\lambda_i - q_i|/\lambda_i$, $i \in \{E_T \quad g_T\}$. The observation noise intensity D will follow a uniform distribution on $[-D, D]$. Fig. 4(c) illustrated that the normalized absolute error of the parameter E_T estimated by the combined method is relatively low. When D is small, the E_T normalized absolute errors estimated by the combined method and the UKF are about the same, slightly larger than the errors estimated by the synchronization-based method. While the noise intensity increases and over the period from 0.06 to 0.1, the normalized absolute error estimated by the combined method grows down distinctly and becomes the lowest one, which represents the robustness to the increased noise intensity and the high estimation accuracy. While the normalized absolute error of the UKF method fluctuates within a certain small band $[0.006, 0.008]$ and remains nearly unchanged broadly except at zero noise intensity where the error reaches up to 0.016, because the UKF works in a noisy environment, it cannot perform well without noise. Conversely, the normalized absolute error E_T of the synchronization-based method increases sharply, meaning that it may fail to estimate the parameters well while noise grows strong.

Fig. 5 shows the estimation results of the low-threshold T-type Ca^{2+} maximum channel conductance. Apparently, in Fig. 5(a), when $D = 0.1$ the convergence of the combined method is slower than the synchronization-based method, and less smooth, although some spike fluctuations which are caused by the effects of the noise and the external periodic current stimulus occurs in the inset chart of the synchronization-based convergence. Besides, it is much more rapid and smooth than the UKF.

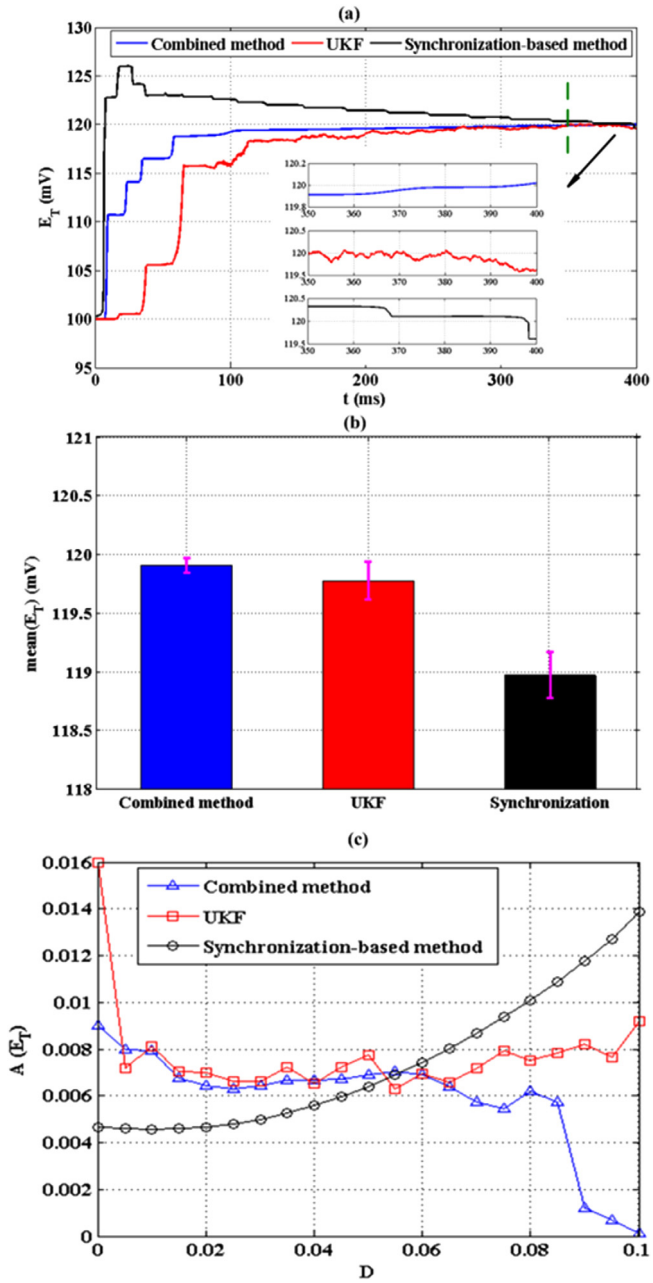

FIG. 4. The results of the unknown parameter E_T estimated from the noise-corrupted time series. (a) The comparison of the results estimated by the three methods when the noise intensity for $D = 0.1$. The inset chart is the enlargement of the estimated results in the last 50 ms. (b) The quantitative comparison after convergence of the three methods. (c) The normalized absolute error of the three methods when the observation noise intensity D changes from 0 to 0.1.

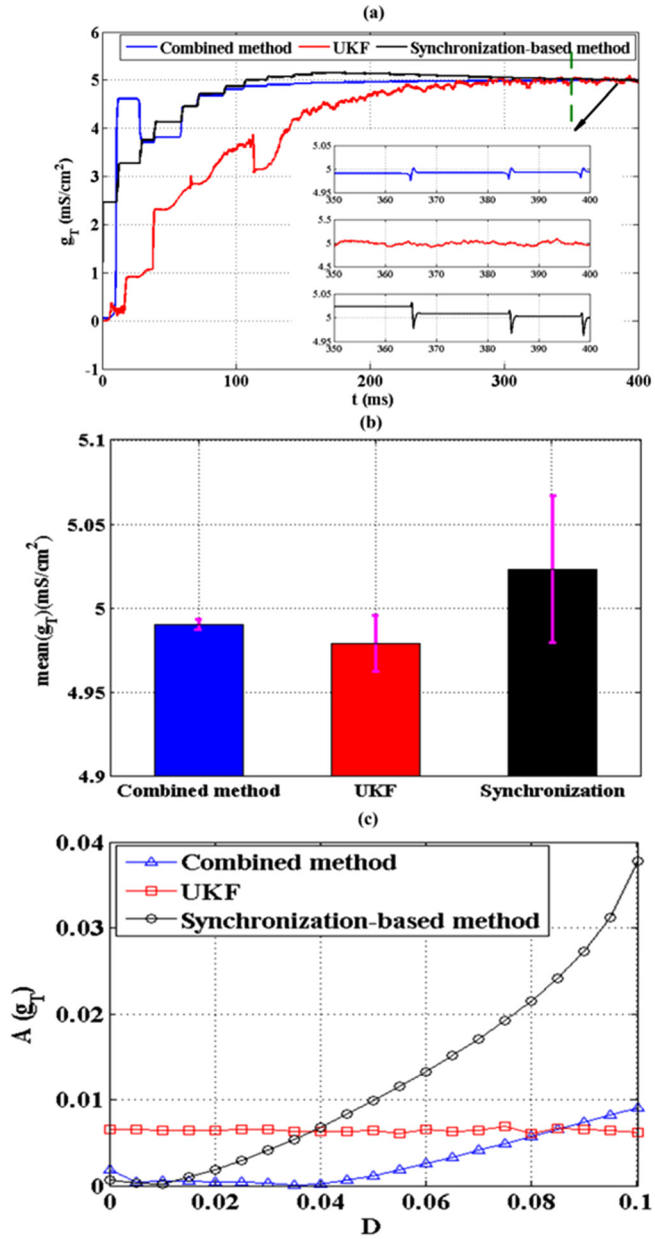

FIG. 5. The results of the unknown parameter g_T estimated from the noise-corrupted time series. (a) The comparison of the results estimated by the three methods when the noise intensity for $D = 0.1$. The inset chart is the enlargement of the estimated results in the last 50 ms. (b) The quantitative comparison after convergence of the three methods. (c) The normalized absolute error of the three methods when the observation noise intensity D changes from 0 to 0.1.

The quantitative comparison of the three methods after convergence shown in Fig. 5(b) illustrates that the estimated average value of the combined method is the nearest to the fixed value with the shortest length of the error bar. So we can make a conclusion similar to Fig. 5(a), that among the three estimation methods, the accuracy of the combined method is the highest and the fluctuation range is minimum.

Fig. 5(c) illustrates the normalized absolute errors along with the increased observation noise D. When D rises, the normalized absolute error of the combined method is lower than the synchronization-based method except near $D = 0$, and its upward trend is far less dramatically, showing a high estimation accuracy and good robustness. When D varies from 0.08 to 0.1, the normalized absolute error of the combined method is slightly larger than the UKF method, the error of which remains in general unchanged when D increases.

In summary, three conclusions can be drawn from Figs. 4 and 5. First, undetermined parameters of the combined method can converge to the true values rapidly with a higher accuracy, and the dynamic performance of this combined method is better than the other two estimation methods. Second, quantitative index shows that the accuracy of

the combined method is the highest and the fluctuations in the estimation process are the smallest. Finally, the robustness against the increased noise intensity of the combined method is the strongest.

The estimation results of other ionic channels have similar performance to the estimation of the low-threshold T-type Ca^{2+} channel (data not shown), which confirms the validity of the combined method for TC model parameter estimation.

V. CONCLUSIONS

The TC neuron model is an important component of Parkinson's disease, but it is worthwhile to note that not all states and parameters of the model could be measured. In this paper, we have adopted an effective estimation method combined the UKF and the synchronization-based adaptive feedback method to estimate the undetermined key parameters of the TC model, such as the maximum ionic conductance and equilibrium reversal potential of the low-threshold T-type Ca^{2+} channel. In the combined method, the noises are first filtered out and state variables without noise are estimated through the UKF algorithm. Then the estimated states are brought into the synchronization-based estimation system to drive the auxiliary system in order to estimate the unknown parameters, so the undetermined parameters can converge to the expected value fast and precisely by adjusting the adaptive rate. Numerical simulations demonstrate that the combined method of which the higher accuracy of parameter estimation and the better robustness to noise can be guaranteed is more effective than only the strategy of the UKF or the synchronization-based method.

Using the combined method to estimate the undetermined parameters of the neuronal model may be considered as a good foundation of further exploring the model dynamics of the Parkinsonian state, especially when a critical parameter characterizing Parkinsonian brain may be immeasurable. Then the critical parameter estimated will be used as the feedback variable in DBS closed-loop strategy. We expect our estimation results will be helpful for further Parkinson's disease analysis.

ACKNOWLEDGMENTS

This work was supported by the National Natural Science Foundation of China (Grant Nos. 61072012 and 61172009), the Tianjin Municipal Natural Science Foundation (No. 12JCZDJC21100), and the China Postdoctoral Science Foundation (Grant No. 2012M510750).

[1]S. J. Schiff, Philos. Trans. R. Soc. London, Ser. A **368**(1918), 2269 (2010).
[2]M. Magnin, A. Morel, and D. Jeanmonod, Neuroscience **96**(3), 549 (2000).
[3]J. Liu, H. K. Khalil, and K. G. Oweiss, J. Neural Eng. **8**(4), 045002 (2011).
[4]J. E. Rubin, C. C. McIntyre, R. S. Turner, and T. Wichmann, Eur. J. Neurosci. **36**, 2213 (2012).
[5]D. Terman, J. E. Rubin, A. C. Yew, and C. J. Wilson, J. Neurosci. **22**(7), 2963 (2002).
[6]M. Anderson, N. Postpuna, and M. Ruffo, J. Neurophysiol. **89**(2), 1150 (2002).
[7]D. S. Andres, D. Cerquetti, and M. Merello, Int. J. Neural Syst. **21**(3), 175 (2011).
[8]P. J. Hahn and C. C. McIntyre, J. Comput. Neurosci. **28**(3), 425 (2010).
[9]M. Pirini, L. Rocchi, M. Sensi, and L. Chiari, J. Comput. Neurosci. **26**(1), 91 (2009).
[10]J. Modolo, E. Mosekilde, and A. Beuter, J. Physiol. (Paris) **101**(1–3), 56 (2007).
[11]E. B. Montgomery and J. T. Gale, Neurosci. Biobehav. Rev. **32**(3), 388 (2008).
[12]S. Santaniello, G. Fiengo, L. Glielmo, and W. M. Grill, IEEE Trans. Neural Syst. Rehabil. Eng. **19**(1), 15 (2011).
[13]X. Feng, B. Greenwald, H. Rabitz, E. S. Brown, and R. Kosut, Neural Eng. **4**(2), L14 (2007).
[14]R. Llinas and H. Jahnsen, Nature **297**, 406 (1982).
[15]H. G. Meijer, M. Krupa, H. Cagnan, M. A. Lourens, T. Heida, H. C. Martens, L. J. Bour, and S. A. van Gils, Neural Eng. **8**(6), 066005 (2011).
[16]Y. Guo and J. E. Rubin, Neural Networks **24**, 602 (2011).
[17]J. Rubin and D. Terman, J. Comput. Neurosci. **16**(3), 211 (2004).
[18]P. Mullowney and S. Iyengar, J. Comput. Neurosci. **24**, 179 (2008).
[19]K. Gautam, A. Vikram, N. V. Thakor, M. H. Schieber, and M. V. Kothare, in American Control Conference (ACC), 2010, p. 53.
[20]L. Buhry, F. Grassia, A. Giremus, E. Grivel, and S. Renaud, Neural Comput. **23**, 2599 (2011).
[21]A. C. Jensen and S. Ditlevsen, Phys. Rev. E **86**, 041114 (2012).
[22]B. Deng, J. Wang, and Y. Q. Che, Chaos **19**, 015105 (2009).
[23]R. Konnur, Phys. Rev. E **67**, 027204 (2003).
[24]Y. Mao, W. Tang, and Y. Liu, Cogn. Process **10**(Suppl 1), S41 (2009).
[25]J. Wang, T. Zhang, and Y. Q. Che, Chaos Solit. Fract. **34**, 839 (2007).
[26]C. H. Jia, J. Wang, and B. Deng, in the 30th Chinese Control Conference (CCC), 2011.
[27]U. Parlitz, L. Junge, and L. Kocarev, Phys. Rev. E **54**, 6253 (1996).
[28]A. Maybhate and R. E. Amritkar, Phys. Rev. E **59**, 284 (1999).
[29]D. Huang, Phys. Rev. E **73**, 066204 (2006).
[30]H. Dedieu and M. J. Ogorzalek, IEEE Trans. Circuits Syst. **44**, 948 (1997).
[31]D. Henry, I. Abarbanel, D. R. Creveling, and J. M. Jeanne, Phys. Rev. E **77**, 016208 (2008).
[32]S. J. Julier and J. K. Uhlmann, Proc. SPIE **3068**, 182 (1997).
[33]G. Ullah and S. J. Schiff, PLoS Comput. Biol. **6**(5), e1000776 (2010).
[34]H. U. Voss, J. Timmer, and J. Kurths, Int. J. Bifurcation Chaos **14**(6), 1905 (2004).
[35]S. J. Schiff and T. Sauer, J. Neural Eng. **5**(1), 1 (2008).
[36]S. J. Schiff, X. Huang, and J. Y. Wu, Phys. Rev. Lett. **98**, 178102 (2007).
[37]F. Kwasniok, Phys. Rev. E **86**, 036214 (2012).
[38]G. G. Rodrigues, U. S. Freitas, D. Bounoiare, L. A. Aguirre, and C. Letellier, IEEE Trans. Biomed. Eng. **60**(5), 1234 (2013).